THE INFLUENCE OF LAND USE CHANGE ON GLOBAL-SCALE FLUXES OF CARBON FROM TERRESTRIAL ECOSYSTEMS

P. E. LEVY[1], A. D. FRIEND[2], A. WHITE[3] and M. G. R. CANNELL[1]

[1]*Centre for Ecology and Hydrology, Bush Estate, Penicuik, Midlothian EH26 0QB, U.K.*
E-mail: plevy@ceh.ac.uk
[2]*NASA GISS, 2880 Broadway, New York NY 10025, U.S.A.*
[3]*Department of Mathematics, Heriot-Watt University, Edinburgh EH14 4AS, U.K.*

Abstract. A process-based approach to modelling the effects of land use change and climate change on the carbon balance of terrestrial ecosystems was applied at global scale. Simulations were run both with and without land use change. In the absence of land use change between 1700 and 1990, carbon storage in terrestrial ecosystems was predicted to increase by 145 Pg C. When land use change was represented during this period, terrestrial ecosystems became a net source of 97 Pg C. Land use change was directly responsible for a flux of 222 Pg C, slightly higher but close to estimates from other studies. The model was then run between 1990 and 2100 with a climate simulated by a GCM. Simulations were run with three land use change scenarios: 1. no land use change; 2. land use change specified by the SRES B2 scenario, and; 3. land use change scaled with population change in the B2 scenario. In the first two simulations with no or limited land use change, the net terrestrial carbon sink was substantial (358 and 257 Pg C, respectively). However, with the population-based land-use change scenario, the losses of carbon through land use change were close to the carbon gains through enhanced net ecosystem productivity, resulting in a net sink near zero. Future changes in land use are highly uncertain, but will have a large impact on the future terrestrial carbon balance. This study attempts to provide some bounds on how land use change may affect the carbon sink over the next century.

1. Introduction

Emissions of carbon resulting from changes in land use comprise a substantial term in the global carbon cycle. The major land use change which affects the terrestrial carbon balance is the clearance of forest for agricultural use. It is estimated that one sixth of the naturally occurring forest area has been cleared to date (Waring and Running, 1998). To a substantial degree, estimates of emissions from land use change determine the estimated size of the so-called "missing sink" in the contemporary global carbon balance. This missing sink is the residual term remaining after the recognised sinks and sources have been accounted for. Emissions from land use change are the most uncertain of the recognised sources, and largely determine the residual. The missing sink is usually attributed to terrestrial vegetation (Keeling et al., 1996; Ciais et al., 1995), and there is considerable interest in how this may change over the next century because of changing climate and CO_2 concentration.

Climatic Change **67:** 185–209, 2004.

The main approach in estimating the role of land use change in the global carbon balance has been a simple "book-keeping" approach, in which statistics on deforestation are combined with estimates of the vegetation carbon content (Houghton et al., 1983; Houghton, 1995). The approach uses generic time-dependent functions for carbon gain and loss in different ecosystem types following conversion of forest to cultivated land and vice versa, and makes no inference about fluxes from vegetation except those arising from land use change.

Recently, attempts have been made to quantify the global land use change flux (LUCF) with more sophisticated methodologies. DeFries et al. (1999) compared the current distribution of vegetation, determined using ground-based and/or remotely sensed data, with model predictions of pre-industrial vegetation, and attributed the difference to land use change. McGuire et al. (2001) incorporated the algorithms of Houghton et al. (1983) into four process-based terrestrial biosphere models to track global carbon fluxes. This has the advantage of simultaneously considering the interacting factors which affect the terrestrial carbon balance, which cannot be rigorously analysed in isolation.

This paper describes the application of this approach to one of the most sophisticated process-based dynamic global vegetation models, 'Hybrid' (Friend et al., 1997). The model has previously been used to quantify the current and future role of terrestrial ecosystems as sinks for carbon (Cramer, 2001; White et al., 1999; White et al., 2000), but simulating 'potential' vegetation which would exist in the absence of human-induced land use change. Here we analyse the response to climate change based on knowledge of physiological processes, whilst modifying the vegetation represented to account for land use change. The aim was to estimate global-scale fluxes of carbon from vegetation arising from changes in land use and climate, using a process-based approach so that future climate scenarios could be included.

The model was first evaluated by simulating changes in vegetation and soil carbon following clearing a South American rainforest. Model predictions were compared with those using the empirical approach of Houghton (1991) and Houghton and Hackler (1995). The model was then run over the historical period at global scale with a climate simulated by the U.K. Hadley Centre Global Climate Model (HadCM3, Gordon, et al., 2000), both with and without land use change (LUC). The model run with land use change was extended to 2100 using three contrasting land use change scenarios and the climate simulated by HadCM3 for the B2 scenario from the IPCC Special Report on Emissions Scenarios (SRES, IPCC, 2000).

2. Model Description

2.1. OVERVIEW

A process-based model of carbon fixation and flow in vegetation and soil was constructed, simplifying the Hybrid model described elsewhere (Friend et al., 1997;

White et al., 2000; Friend and White, 2000). The new model, termed 'HyLand', operated on a daily time-step and included simplified hydrology and N dynamics. Inputs were climate, atmospheric CO_2, and land use change through time. Outputs were vegetation and soil carbon pool sizes and terrestrial-atmosphere carbon fluxes. Three vegetation types were represented: herbs, broadleaved and needleleaved trees. Deforestation and cropping altered the flows of carbon between vegetation, soil and atmospheric pools. Further model details are given in appendix and Table A1.

2.2. VEGETATION

Absorption of photosynthetically active radiation (PAR) by the canopy was modelled using Beer's Law (Equations A1 and A2). Daily tree canopy photosynthesis was calculated assuming that photosynthesis and foliage N content declined down the canopy at the same rate as photosynthetically active radiation (PAR) (Sellers et al., 1992; Equation A3). The model was particularly sensitive to the nitrogen content of the top layer of foliage (N_{top}) (see Parameter optimisation). The rate of photosynthesis of the top layer was calculated from foliar N content, stomatal conductance, temperature, PAR and foliar CO_2 concentration, using the biochemical model of Farquhar and von Caemmerer (1982) as described previously Friend et al. (1997). Stomatal conductance was calculated from foliar N content, temperature, PAR and CO_2 concentration, plus soil water potential, using the empirical Stewart-Jarvis model as parameterised by Friend et al. (1997). Herbs, broadleaved and needle-leaved trees were given different photosynthetic parameters as in White et al. (2000), except for the N content of the top layer of foliage.

Maintenance respiration (i.e. respiration not accounted for in net daytime photosynthesis) was assumed to be a constant fraction of gross photosynthesis (Equation A4), as suggested by several recent studies (Gifford, 1995; Waring et al., 1998; Dewar et al., 1999). This is in contrast to the assumption in previous versions of the Hybrid model, in which maintenance respiration was a linear function of the total carbon content of each of the plant compartments and an exponential function of air temperature (Ryan, 1991). Which of these assumptions is more correct remains a contentious issue (Thornley and Cannell, 2000).

Net primary productivity (NPP, equivalent to whole plant growth) of the herbaceous layer was calculated as for the woody layer, except that it depended, not only on N content, but also on the LAI of the woody plant canopy layer above (Equation A2). NPP was allocated annually in fixed ratios to foliage, stem and roots. Leaf area index was the product of foliage carbon and specific leaf area. Litter fall was calculated from fixed turnover rates.

All three vegetation types were initiated each year and, because of their different parameters, grew at different rates and competed for light. Herbs dominated if the woody canopy was sparse. If the stem carbon of one tree type was within $\pm 50\%$ of that of the other, then PAR was shared equally; if not, the lesser type

was excluded. All plant types were initialised at 0.1 kg C m^{-2} allocated between compartments with the same fractions as for NPP. Parameters values are listed in Table A1.

2.3. SOIL

The flux of water to the soil was the difference between precipitation and evaporation. The latter was calculated by resolving the isothermal energy balance for sensible heat to obtain the surface temperature and then employing the Penman-Monteith equation (Equations A5–A7). When the soil contained 10% more than its capacity there was drainage. Soil water-filled space was calculated from soil water content and a prescribed soil texture as described by Friend and White (2000). Soil water potential was calculated from soil water holding capacity, which was assumed to be a function of soil carbon (Friend and White, 2000; Equation A8).

Decomposition of soil organic carbon was simulated using the Century model of Parton et al. (1987) as adapted by Comins and McMurtrie (1993) and fully described by Friend et al. (1997). The rate of decomposition was a function of soil water potential and temperature. The soil was divided into an upper layer of 20 cm and a lower layer of 80 cm. Carbon moved from the top 'decomposable' soil to the lower 'protected' layer of organic matter at prescribed rates, which were tuned to give constant pool sizes with depth. In order to deal effectively with deforestation, pools of coarse surface and below-ground structural litter were added to the model of Friend et al. (1997) with residence times of 73 and 53 years, respectively, when soil temperature and moisture factors were unity. These long residence times delayed carbon loss after clearfelling. Since soil carbon may take centuries to reach equilibrium, the pool size was initialised at the start of the spin-up phase with an estimated soil carbon content derived from the observed relationship between soil carbon and pre-industrial precipitation and temperature (Friend and White, 2000).

2.4. LAND USE

Three land use options were employed, which were assumed to alter carbon fluxes as follows.

Undisturbed vegetation. No alterations: the carbon content of the three possible vegetation types and their associated soil varied dynamically with the climate and atmospheric CO_2 concentration.

Deforestation (*clearfelled forest*). (i) It was assumed that 64% of the above-ground stem carbon was removed instantly. Houghton (1991) assumed that 33% of the original vegetation was left to decay on site at the time of clearing; thus 67% was lost to burning or removal. If 30% of stem mass is stump and below-ground and all fine plus 30% of coarse above-ground litter is burned (Hao et al., 1990), then about

64% of above-ground stem must be removed to leave 33% of the original carbon on site (70% of stem is assumed to be coarse). (ii) Clear-cutting was immediately followed by a fire, which oxidized 30% of coarse above-ground stem litter, all other litter, and all above-ground herbaceous plant parts (Hao et al., 1990). Charcoal production and timber product pools were not represented. (iii) The remaining litter was apportioned to coarse and fine litter above- and below-ground. (iv) Soil disturbance in the year of deforestation was assumed to cause 30% of the carbon in protected pools to move to the active decomposable pools.

Cropland. (i) Tree regeneration was prevented. (ii) Cultivation caused 30% of the carbon in protected pools to move to the active decomposable pools every year. (iii) Harvesting removed 50% of above-ground vegetation carbon every year. The remaining carbon was transferred to litter. (iv) Incorporation of litter was simulated by assuming that 50% of the above-ground structural and metabolic litter pools were transferred to the topsoil structural and metabolic litter pools each year of cultivation. (Voroney and Angers, 1995; van Veen and Kuikman, 1990).

3. Model Evaluation for a South American Rain Forest

Deforestation of tropical rainforest is currently the largest component of the global flux of carbon from land use change (Houghton and Hackler, 1999). To evaluate the model for this situation, predictions of changes in vegetation and soil carbon following clearance of a tropical rainforest were compared with the empirical response curves derived by calibrating rates of change with observations (Houghton et al., 1991).

3.1. CLIMATE AND LAND USE SCENARIOS

The model was run in a constant climate with 25 °C, a 12-hour day with 1500 μmol (photons) m^{-2} s^{-1} PAR, 360 ppm CO_2, 500 Pa air vapour pressure deficit and -0.01 MPa soil water potential. The model was first tuned to give equilibrium values of 20 kg C m^{-2} vegetation and 9.8 kg C m^{-2} soil in this climate. These were the values assumed by Houghton et al. (1991) for undisturbed South American rainforest. The N content of the top canopy layer was increased from 1.80 to 1.89 g N m^{-2} and the NPP allocated to foliage from 10 to 20% resulting in an LAI of 10. Soil carbon was tuned by varying the soil-temperature activity factor (Comins and McMurtrie, 1993). Some adjustment of parameter values for the herb layer was necessary to reproduce Houghton's values of 0.5 kg C m^{-2} for cropland, but this had little effect on the large carbon fluxes and soil pool. The model was run to simulate the conversion of a rainforest to cropland, the maintenance of the cropland for 20 years, and then their abandonment allowing the forest to regenerate (Figure 1).

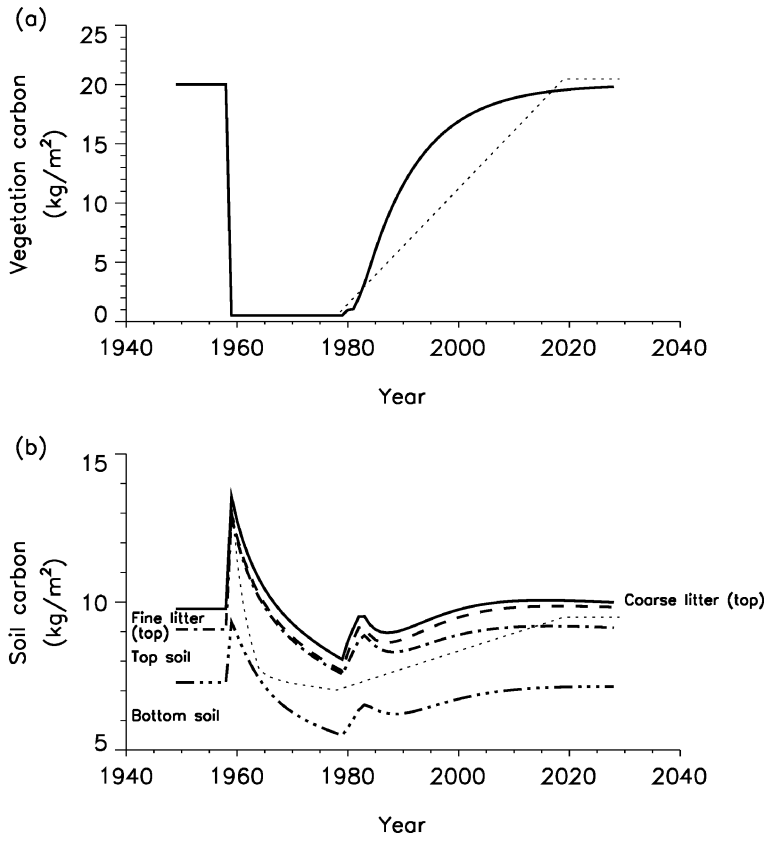

Figure 1. Model predictions of (a) vegetation and (b) soil carbon responses to clearance for cropland followed by abandonment after 20 yr under the environmental conditions listed in text. Soil pools are shown cumulatively, with litter components of the topsoil (including surface litter); total shown by the solid line. Predictions by the bookkeeping approach (see text) shown by small dashes.

3.2. CHANGES IN VEGETATION AND SOIL CARBON

Stemwood removal and burning at clearfelling reduced total site carbon by 53% despite a 39% increase in soil carbon due to root and aboveground litter input from the felled trees (Figure 1). Over the next 10 years, soil organic matter declined, owing to small litter inputs (Figure 1b). Top and bottom soil lost about 40% carbon over 20 years – well within the measured range for South and Central American tropical forests (Houghton et al., 1983; Lugo et al., 1986). However, 69% of the above-ground and 60% of the below-ground coarse litter was still present 20 years after clearfelling. Ten years after clearfelling, cropland had 66% less carbon than the undisturbed forest.

Following abandonment, woody vegetation rapidly re-grew, reaching 95% of its undisturbed carbon after 32 years. The herbaceous layer dominated for three years, but was then shaded-out by the tree layer. This resulted in a sigmoidal response

curve, as sometimes observed (Saldarriaga, 1987; Nepstad et al., 1991) compared with an assumed linear recovery over 20 years by Houghton et al. (1991). The modelled rate of forest growth during early regeneration was about 1 kg C m^{-2} y^{-1} – similar to that of young tropical plantations (Brown et al., 1986). When cropland was abandoned, low levels of soil carbon were initially increased as herbs dominated with high litter inputs (owing to high turnover rates), but then fell as trees regenerated (with a lower litter input) before beginning a slow recovery (Figure 1b). The mean rate of soil carbon accumulation over 50 years after cropping was 0.038 kg C m^{-2} y^{-1} similar to that found by Lugo et al. (1986) in Costa Rica.

The model predicted a much slower decline in soil carbon following clearfelling than Houghton et al. (1991), resulting in over 30% more soil carbon after 10 years (Figure 1b). The reason was that we assumed that woody litter, which comprised 96% of all litter after clearfelling, had turnover times of 73 years aboveground and 53 years belowground, whereas Houghton et al. (1991) assumed that woody litter (slash) turned over in only 2.5 years. Our choice was based on estimates of 61–89-year turnover times for 30–40 cm diameter fallen logs in Oregon (Grier, 1978) and Wyoming (Fahey, 1983) and 9.2 years for 5–33 cm diameter wood in Ghana (John, 1973) – recognising that many logs in rainforests will greatly exceed 30–40 cm in diameter.

3.3. CONCLUSIONS

The model simulated realistic dynamic patterns of loss and gain in vegetation and soil carbon following land use change, well within the few measured values. The rate of loss of soil carbon following deforestation was slower than previously assumed, because coarse woody litter fractions were given long turnover time. Also, forests recovered following a realistic sigmoidal curve, rather than linearly with time. We stress that our process model does not necessarily give more reliable predictions of the effects of land use on vegetation and soil carbon than empirical models – both approaches rely on uncertain assumptions. Its strength is that it tracks carbon within the framework of a dynamic global vegetation model, and so enables land use to be included in predictions of the effects of climate change, as described.

4. Application at Global Scale

The model was run on a global scale between 1700 and 1990, both with and without land use change. The simulation with land use change was extended to 2100 using using three contrasting land use change scenarios and the climate simulated by HadCM3 for the SRES B2 scenario. The B2 scenario was chosen because it was intermediate within the four reference scenarios, in terms of human population

TABLE I
Details of the scenarios for climate, CO_2 and land use change (LUC) used in the global-scale simulations

Simulation	Climate	CO_2	LUC
	1300 to 1699		
Spin-up	Pre-industrial	288	none
	1700 to 1989		
No LUC	Had CM3 simulation	288 to 350	none
With LUC	Had CM3 simulation	288 to 350	R&F
	1990 to 2100		
No LUC	Had CM3 simulation	351 to 614	none
B2 LUC	Had CM3 simulation	351 to 614	From B2 scenario
LUC α Popn	Had CM3 simulation	351 to 614	From population in B2 scenario

R&F = Ramankutty and Foley (1999).

growth, greenhouse gas emissions, CO_2 concentrations and climatic change, and because it was the only reference scenario to include any continued deforestation (the others are considered unrealistic in this respect). Details of the scenarios for climate, CO_2 and land use change (LUC) used in the global-scale simulations are given in Table I. The spatial resolution was determined by the simulated climate from the HadCM3 model, where each grid cell represents 2.5° latitude by 3.75° longitude. At each grid point, ten plots were represented which could have different land use histories. The temporal resolution was one day.

4.1. CLIMATE DATA

For the period 1860 to 1990, climate data (temperature, diurnal temperature range, relative humidity, downward short-wave radiation and precipitation) were taken from the UK Hadley Centre Global Climate Model (HadCM3). For the pre-industrial period before 1860, the HyLand model was run using climate data from the above source for the decade 1860–1869, in a continuous loop. From 1990 to 2100, the HadCM3 simulation corresponding to the B2 SRES emission scenario was used (simulation h3b2b; Johns et al., 2003). Atmospheric CO_2 concentrations were increased annually, taken from the ISAM model conversion of the B2 scenario emissions, reaching 614 ppm by 2100 (IPCC, 2000).

4.2. LAND USE DATA

Data on the historical expansion of cropland were taken from the study of Ramankutty and Foley (1999). These data cover the period 1700–1992 at

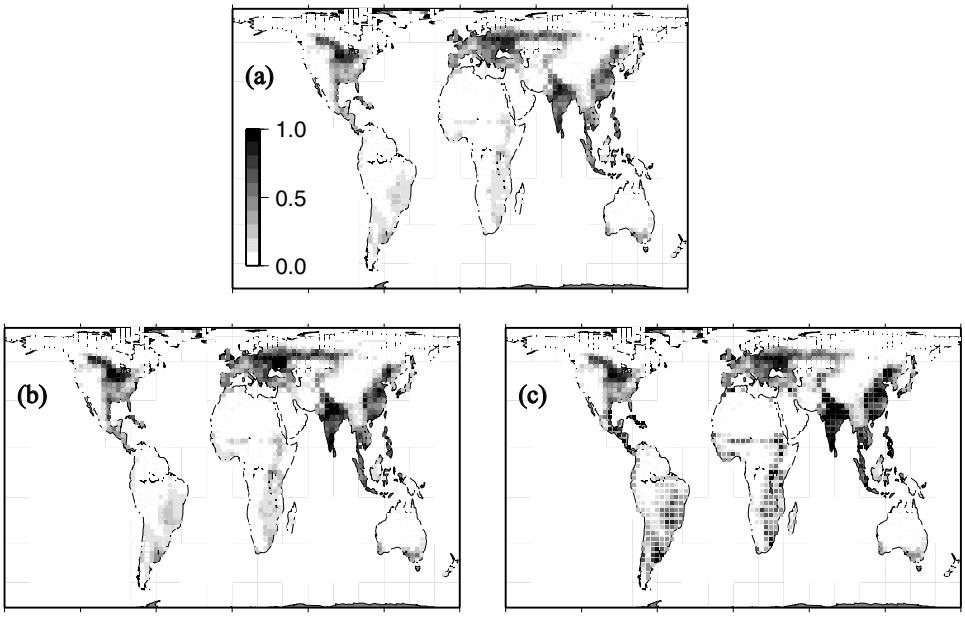

Figure 2. (a) Map of the fraction of land under crops in 1990, from the study of Ramankutty and Foley (1999). (b) and (c) show the fraction of land under crops in 2100, based on the B2 LUC and LUC α Popn scenarios, respectively. In all maps, an equal-area projection is used (cylindrical with a standard parallel of 45° (Peters projection)).

approximately 30-year resolution, and encompass the global land surface at 0.5 degree spatial resolution. These data were aggregated up to the 3.75 × 2.5 degree used by HadCM3 to prescribe the historical course of land use change in the HyLand model. The data show an increase in cropland from around 2% of the global land area in 1700, to over 13% in 1990 (Figure 2a). The timing of land use changes within each 30-year interval was random.

For the period 1990–2100, three scenarios for land use change were used:

1. No LUC – no land use change after 1990;
2. B2 LUC – the change in cropland area was taken directly from the SRES B2 scenario (Figure 2b). The B2 scenario contains estimates of land use at decadal intervals within four socio-economic regions (OECD; Former Soviet Union; Asia; Africa and Latin America). Each decade, the change in the regional cropland coverage was applied to each grid cell within that socio-economic region, i.e.:

$$f_{\text{crop,local},t} = f_{\text{crop,local},1990} \cdot f_{\text{crop,region},t} / f_{\text{crop,region},1990}$$

where $f_{\text{crop,local},t}$ is the local fraction of cropland coverage cropland within a 3.75 × 2.5 degree grid cell at time t, and $f_{\text{crop,region},1990}$ is

the fraction of cropland coverage within the SRES socio-economic region in 1990. The timing of land use changes within each decade was random.

3. LUC α Popn – the change in cropland area was assumed to follow changes in population in the B2 scenario. That is,

$$f_{\text{crop,local},t} = f_{\text{crop,local,1990}} \cdot P_{\text{region},t} / P_{\text{region,1990}}$$

where $P_{\text{region},t}$ is the population in the SRES socio-economic region at time t (other subscripts same as in the previous). Thus, this assumes that the area of cropland required per head of population will remain the same between 1990 and 2100. Although the B2 scenario does predict an increase in cropland area between 1990 and 2100 of 22%, this is small in relation to the change in population, which increases by 97% to 10.4 billion. We therefore use the simplistic assumption that cropland area follows population growth as a 'business as usual' scenario (Uusivuori et al., 2002), as an alternative to the B2 scenario, which may be overly optimistic regarding the land area required for food production. The potential cropland area required in the population-based scenario (Figure 2c) is feasibly available, according to a recent study (Ramankutty et al., 2002). In the B2 scenario, population growth is very small for the two regions that include the industrialized countries. In Asia, the population stabilises at 177% of the 1990 value, whilst in Africa and Latin America, the population reaches 347% of the 1990 value by the end of the 21st century.

4.3. PARAMETER OPTIMISATION

A sensitivity analysis and parameter optimisation exercise was performed on the model. An evolutionary computation approach was used to find the parameter set which best reproduced current estimates of global vegetation carbon, soil carbon and net primary production (target values were 600 Pg C, 1500 Pg C and 70 Pg C y^{-1}, respectively). This was implemented using an evolutionary computation algorithm, the Pareto Optimal Model Assessment Cycle (POMAC, Reynolds and Ford, 1999), in which 15 parameters were allowed to vary within $\pm 20\%$ of the default value. 30 generations were run with a population size of 30 at each step (=900 runs at global scale for the period 1860–1990). The intention was to use the best fitting parameter set from the final generation. However, when a sensitivity analysis was performed, and partial correlation coeffiecients were calculated for each of the parameters and outputs, it was apparent that the N_{top} parameter accounted for much of the variation in the outputs (Figure 3). A very similar result to the optimal parameter set could be achieved using the default parameterisation but setting N_{top} to 1.3 g N m^{-2} (previously 1.8), and this parameterisation was used in all subsequent simulations.

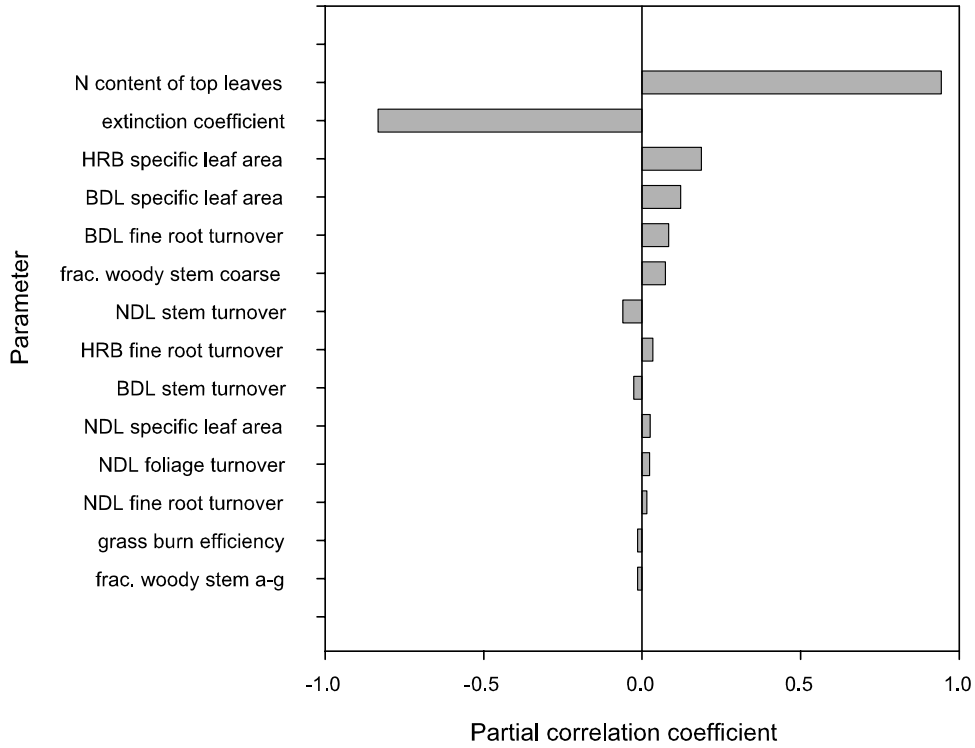

Figure 3. Partial correlation coefficients between 14 model parameters and global vegetation carbon, derived from 900 runs of the model using an evolutionary computation algorithm. Abbreviations are: HRB = herbaceous plants; BDL = broad-leaved plants; NDL = needle-leaved plants; frac = fraction; a-g = above-ground. Other details are in Table A1.

5. Results

5.1. 1700 TO 1990

The behaviour of the model is broadly similar to the more complex Hybrid model (Friend et al., 1997). Figure 4 shows the global distribution of carbon in vegetation in 1990 predicted by the HyLand model including land use change, compared with the ground-based estimates of Olson et al. (1983). HyLand reproduces the broad patterns in biomass, with the local maxima in Amazonia, central Africa and S.E. Asia, and the desert regions of the Sahara, central Asia, western Australia and west of the Andes. The main apparent discrepancy is an overestimation of vegetation in the tropics and an underestimation at northern latitudes. Another discrepancy is the underestimation of forests in the Pacific northwest of North America. Given that the two data sets are entirely independent, the agreement is reasonable, which suggests we can put a degree of confidence in the model's predictive ability.

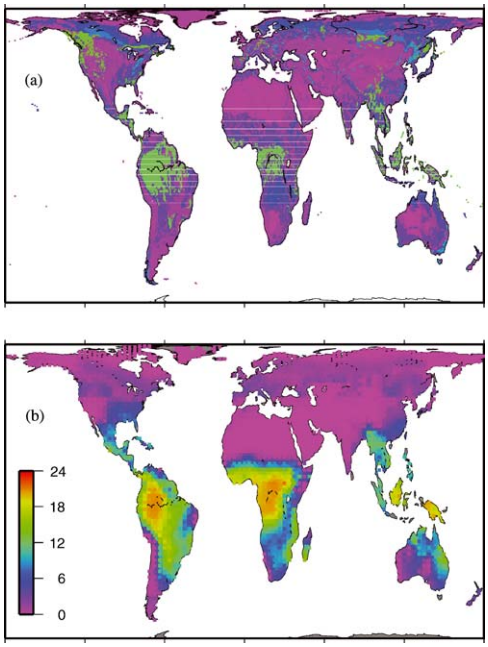

Figure 4. Global distribution of carbon in terrestrial vegetation (a) estimated by Olson et al. (1983) and (b) predicted by the HyLand model in 1990, including land use change. Plotted values are in kg C m^{-2}.

Between 1300 and 1700, under a pre-industrial climate, an equilibrium is reached where NPP equals soil respiration, and the global pools of carbon in vegetation and soil remain constant. Whilst at this equilibrium, net ecosystem productivity (NEP equivalent to NPP minus heterotrophic soil respiration), the flux resulting directly from land use change which bypasses respiration, e.g. by fire and logging (LUCF), and net biome productivity (NBP, equivalent to NEP plus LUCF) are all zero. In the absence of land use change, changes in climate and CO_2 concentration cause NPP to increase from around 71–80 Pg C y^{-1} between 1700 and 1990, and NEP to increase from 0 to 2.3 Pg C y^{-1} (Figure 5), giving a total NEP of 145 Pg over this period (Table II).

When land use change is introduced in 1700, NPP is initially reduced at a near-constant rate as the amount of live biomass declines (Figure 6), and LUCF is fairly constant at around -0.4 Pg C y^{-1} (fluxes from the atmosphere to the land are denoted positive throughout). After 1860, the positive effects of climate change and increasing CO_2 concentration cause an increase in NEP, up to approximately $+2$ Pg C y^{-1} in the 1980s. Summed over the period 1700–1990, the NEP term combines with the much larger, negative LUCF term to give an NBP of -97 Pg C (Table II). That is, the terrestrial biosphere is a net source of carbon over this period, and only becomes a net sink during the 1970s.

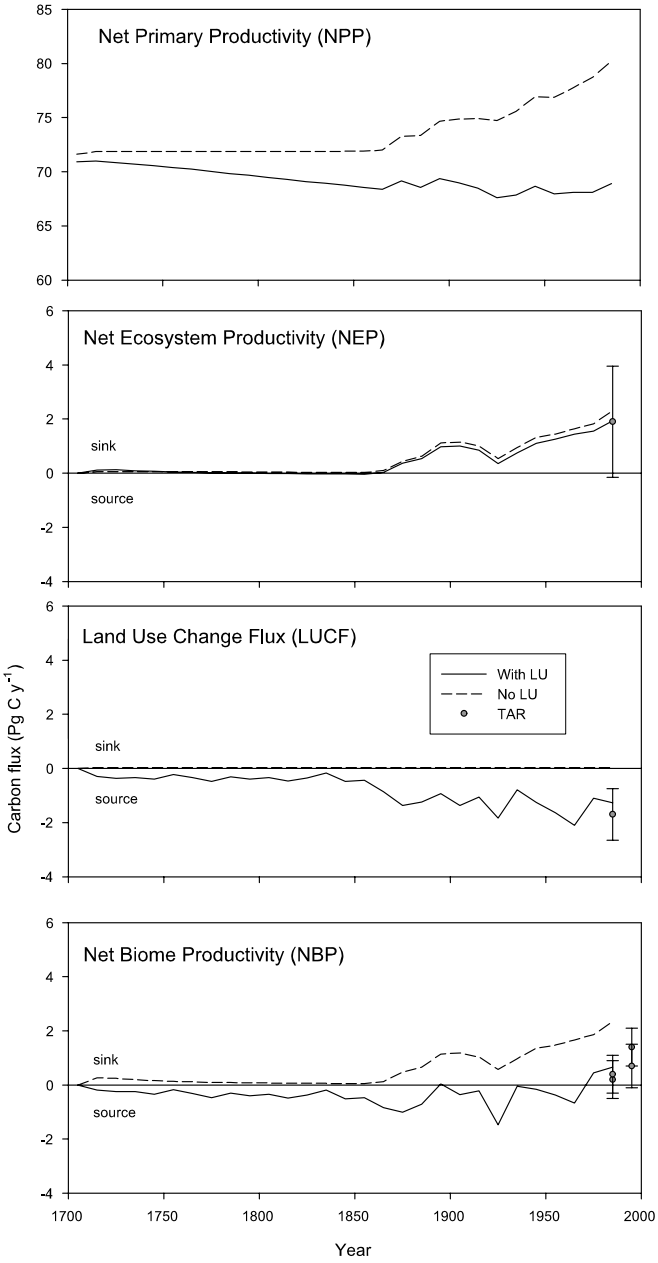

Figure 5. Global fluxes of carbon predicted by HyLand over the historical period, both with and without land use change (LUC). Fluxes shown are net primary productivity (NPP, equivalent to whole plant growth), net ecosystem productivity (NEP equivalent to NPP minus heterotrophic soil respiration), the flux resulting directly from land use change (LUCF), and net biome productivity (NBP, equivalent to NEP plus LUCF). Fluxes from the atmosphere to the land are denoted positive throughout. Also shown are independent values based on inverse modelling of trends in atmospheric CO_2 and O_2 concentrations from the Third Assessment Report of the IPCC (TAR, Prentice, 2001).

TABLE II

Change in carbon storage in terrestrial ecosystems (vegetation plus soil) predicted by the HyLand model

	NEP	LUCF	NBP
	1700 to 1849		
No LUC	0.0	0.0	0.0
With LUC	3.7 (0.02)	−49.6 (−0.3)	−45.9 (−0.3)
	1850 to 1989		
No LUC	144.7 (1.0)	144.7 (1.0)	144.7 (1.0)
With LUC	121.3 (0.9)	121.3 (0.9)	121.3 (0.9)
	1700 to 1989		
No LUC	144.7 (1.0)	0.0	144.7 (1.0)
With LUC	125.1 (0.4)	−222.3 (−0.8)	−97.3 (−0.3)
	1990 to 2100		
No LUC	358.1 (3.2)	0.0	358.1 (3.2)
With B2 LUC	331.8 (3.0)	−74.9 (−0.7)	257.0 (2.3)
LUC α Popn.	296.5 (2.7)	−290.2 (−2.6)	6.2 (0.06)

Abbreviations are as follows: NEP: net ecosystem productivity (equivalent to NPP minus heterotrophic soil respiration); LUCF: land use change flux (which bypasses respiration, e.g. by fire and logging; and NBP: net biome productivity (equivalent to NEP plus LUCF). Values are totals in Pg C followed by mean rates in Pg C y^{-1} in parentheses. When there is no land use change, NBP equals NEP. Fluxes from the atmosphere to the land are denoted positive.

Figure 7 shows the distribution of the change in carbon in vegetation in between 1850 and 1990. In the absence of land use change, vegetation biomass increases across the globe, approximately in proportion to the initial biomass, but with additional increases in dry areas such as central Australia, where the effect of elevated CO_2 alleviates the effect of water stress. When land use change is incorporated in the model, a reduction in total carbon occurs throughout the populous regions: USA, Europe, India and China, as well as regions of sub-Saharan Africa and South America.

5.2. 1990 TO 2100

In the scenarios where future changes in land use are small (B2 LUC) or zero (No LUC), NPP and the vegetation C pool increase almost linearly between 1990 and 2090 (Figures 8 and 9). NEP reaches a peak of around 4 Pg C y^{-1} in 2020. Thereafter, the negative effects of changes in climate increase to a similar magnitude to the positive effect of CO_2 fertilisation, and NEP then declines to near zero by 2100 (Figure 8). Summed over the period 1990–2100, NBP is positive in both B2 LUC and No LUC scenarios, with means of 2.3 and 3.2 Pg C y^{-1} (Table II).

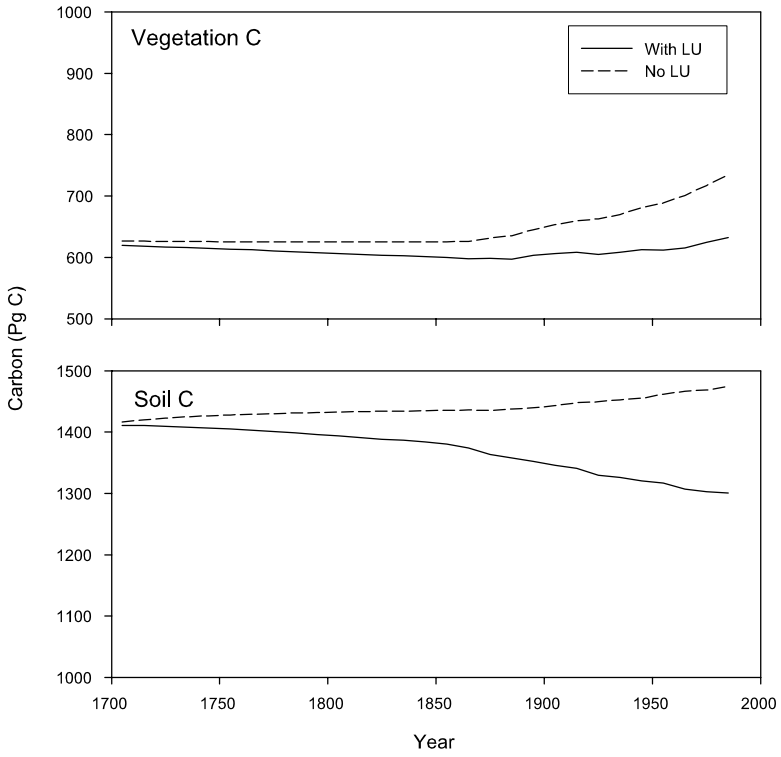

Figure 6. Global stocks of carbon in vegetation and soil predicted by HyLand over the historical period, both with and without land use change.

In the scenario where land use change is based on population change (LUC α Popn), a much larger LUCF is produced, peaking at -4.3 Pg C y^{-1} in 2010 and declining thereafter as population growth slows (Figure 8). This reduces the increase in NPP and the vegetation C pool, and results in a decrease in the soil C pool (Figure 9). The net result is that NBP is negative until the 2050s. When summed over the period 1990–2100, NBP is near zero (0.06 Pg C y^{-1}, Table II).

Figure 10 shows the geographic distribution of the change in terrestrial carbon storage between 1990 and 2100. In the scenarios where future changes in land use are small or zero (Figures 10a and 10b), the carbon sink is distributed widely, with most regions across the globe accumulating carbon. The major exception is the region around the Amazon basin, which is predicted to be a net source over this period. This is because of changes in temperature and rainfall, with HadCM3 predicting considerable warming and drying over this area. In the LUC α Popn scenario, source areas are widespread throughout the tropics, where the expansion in population and cultivated land in the developing countries is predicted (Figure 10c). Much of South and Central America, sub-Saharan Africa and South East Asia become carbon sources in this scenario.

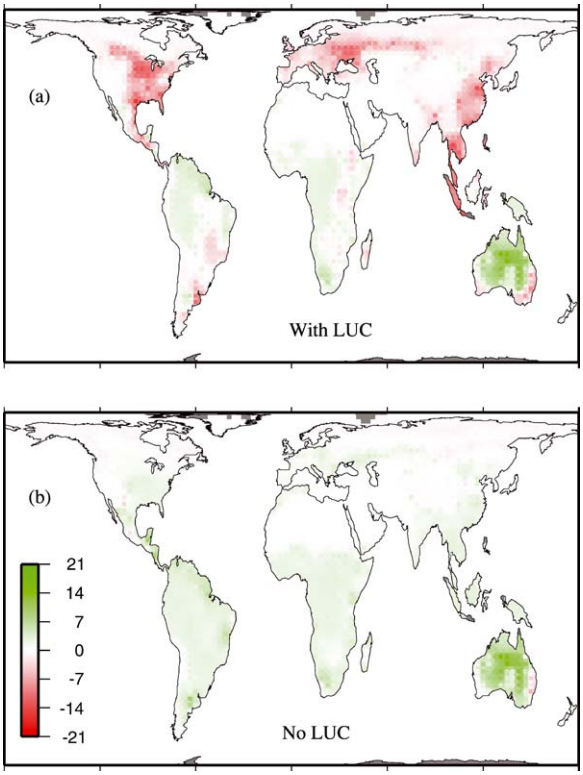

Figure 7. Global distribution of the change in total ecosystem carbon (vegetation plus soil) between 1850 and 1990 predicted by the HyLand model, both with and without land use change. Plotted values are in kg C m^{-2}.

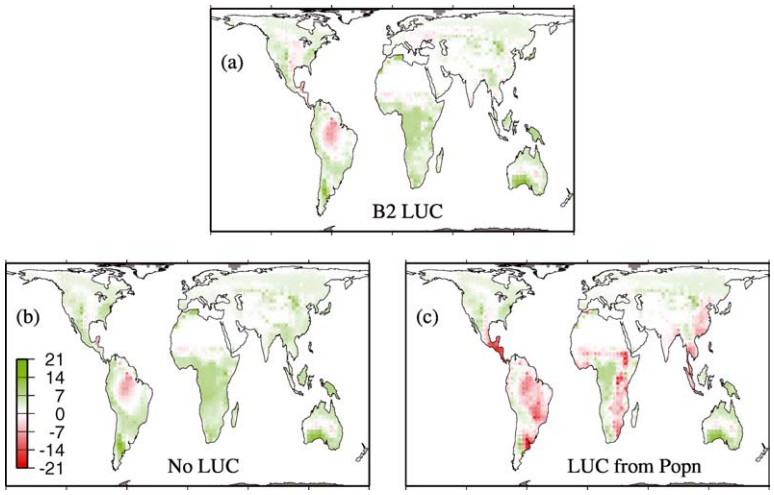

Figure 10. Global distribution of the change in total ecosystem carbon between 1990 and 2100 predicted by the HyLand model, both with and without land use change. Plotted values are in kg C m^{-2}.

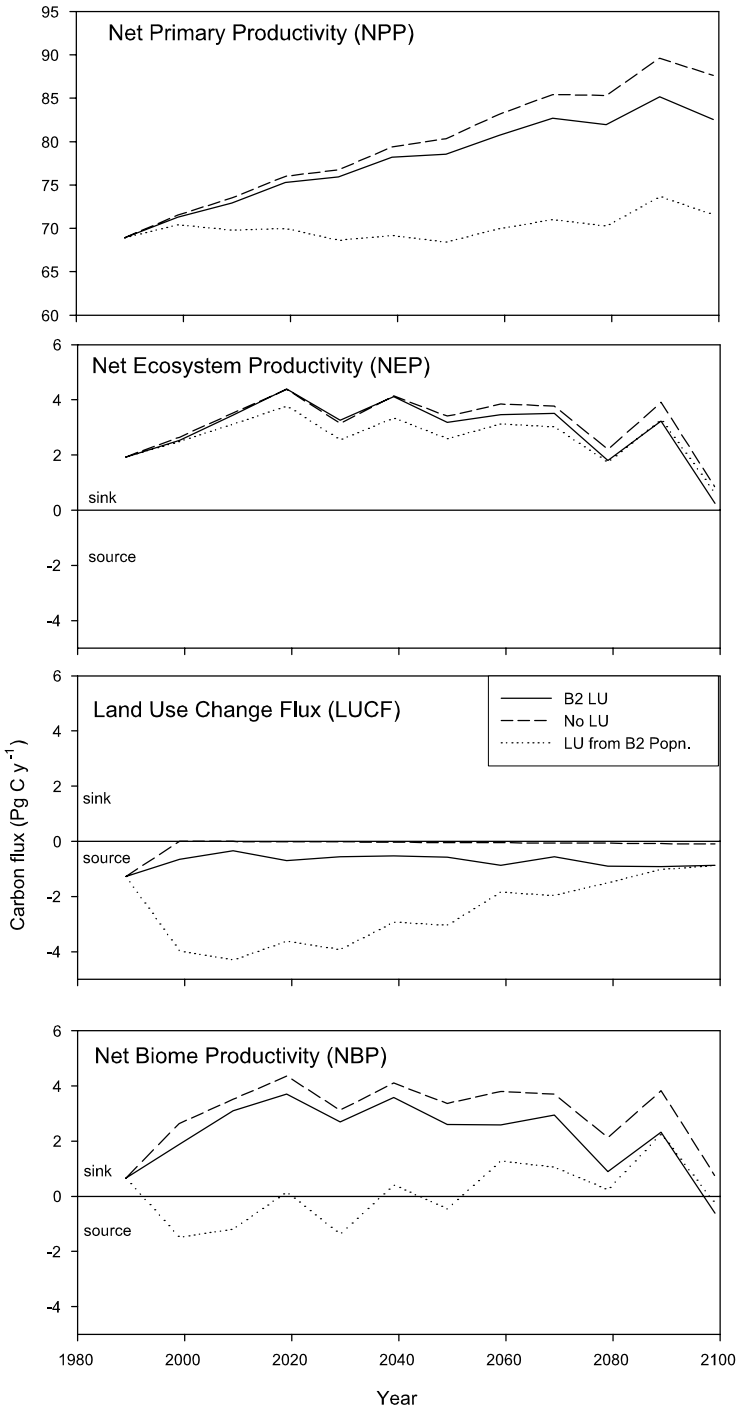

Figure 8. Global fluxes of carbon predicted by HyLand over the 21st century, both with and without land use change.

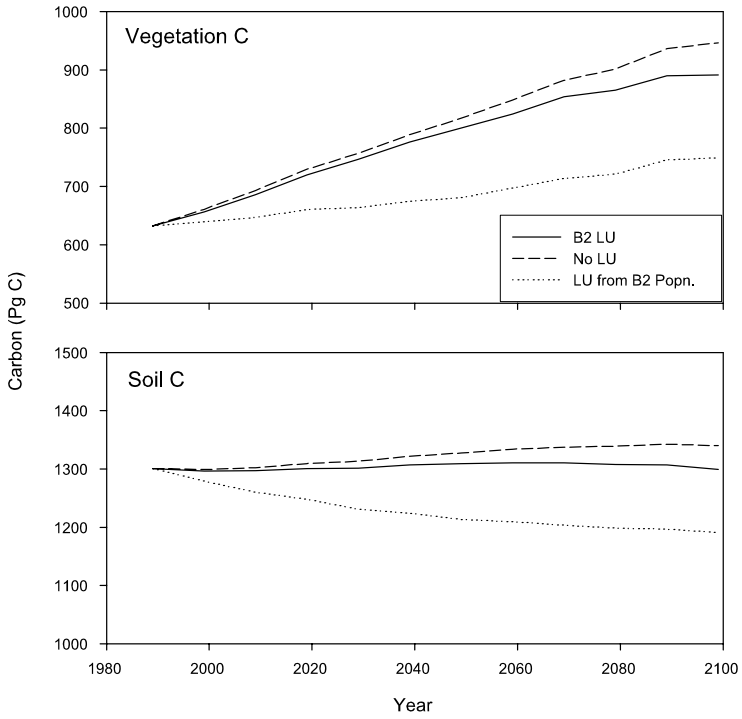

Figure 9. Global stocks of carbon in vegetation and soil predicted by HyLand over the 21st century, both with and without land use change.

6. Discussion

Our estimates of the land use change flux from the historical simulations can be compared with three other studies (Table III). The values obtained in this study are somewhat higher in all cases, though a reason for a systematic difference is not obvious. One possibility is that our model has a bias towards overestimating tropical vegetation and underestimating boreal vegetation. As a substantial fraction of the deforestation occurred in tropical regions (Figure 7), this would lead to

TABLE III
Comparison of estimates of the flux from land use change (LUCF, Pg C y^{-1}) from this and other global-scale studies

Time period	Study	LUCF	LUCF, this study
1700–1990	DeFries et al. (1999)	−191	−222
1850–1990	Houghton (1999)	−124	−173
1920–1990	McGuire et al. (2001)	−56 to −91	−100

an overestimation of the LUCF. We note that McGuire et al. (2001), using four models and a similar method as here, obtained values with a range of 35 Pg (46% of the mean), so a considerable degree of variability between models is to be expected. Our model was run using a simulated climate from the HadCM3, not the observed climatology as used by McGuire et al. (2001), and this is likely to introduce discrepancies between model predictions.

Another possible source of discrepancies between models is the allocation of necromass produced by land use change between combustion and decomposition, as this determines whether it is counted in the NEP or LUCF terms. NEP would be increased and LUCF made more negative if a greater fraction of necromass were burnt off rather than respired. However, the variation in this fraction with different types of land use change and different soil types is highly variable, and this is a large uncertainty in the partitioning between the NEP or LUCF terms.

Comparing our NBP value for the 1980s (the most recent decade for which complete land use data are available) with those collated by Prentice et al. (2001) gives values of 0.6 and 0.2 ($\pm\sigma = 0.7$) Pg C y^{-1}, respectively. Our NBP estimate is therefore high but within the error interval, and some individual inversion studies give higher values (e.g. Gurney et al., 2002). Note that the NBP estimate from our study is not imposed on the model *a priori*, as the N_{top} parameter was only tuned to achieve realistic values of current vegetation and soil pools and NPP.

Figures 8–10 demonstrate that the land use change scenario has a considerable impact on predictions of the future terrestrial carbon sink. In the LUC α Popn scenario, 290 Pg is released by land use change between 1990 and 2100; that is, more than was released in the previous three centuries. This LUCF almost entirely offsets the positive NEP attributable to increasing CO_2 and climate change, resulting in a near zero terrestrial carbon sink. The estimate is feasible, given that House et al. (2002) estimated that total deforestation of existing forests would result in a LUCF of 450–820 Pg.

The prediction of future land use change is highly uncertain as it depends on the many socio-economic processes which determine population growth and the requirements for cultivated land. Here we take the approach of taking relatively extreme scenarios and recognising that the actual outcome will probably lie within this range. The LUC α Popn scenario could have been made more extreme by using population growth from the A2 scenario, where population reaches 15 billion by 2100 (IPCC, 2000).

The principal advantage of our approach is the inclusion of land use change in the model whilst retaining dynamic vegetation processes. Thus, actual rather than potential vegetation is represented without it being prescribed statically, and the inclusion of physiological processes permits extrapolation into altered climatic conditions. However, the simulations described here were carried out independently of the HadCM3 climate simulations, and with prescribed CO_2 concentration. There are therefore no feedbacks between changes in the global vegetation and atmosphere. Many such feedbacks are possible and have been demonstrated in various

GCM studies (Martin et al., 1999; Cox et al., 2000; Betts, 2000; Douville et al., 2000). These will increase or decrease the magnitude of the effects predicted here, depending on the balance of positive and negative feedbacks, which is still open to debate. The LUC α Popn simulation would presumably result in a substantially different CO_2 concentration and climate if the models were linked via the carbon cycle.

The effect of land use change on carbon storage is relatively simple compared with the other uncertainties associated with global change. For example, it is possible that the positive effects of climate change on terrestrial carbon storage will be much less than predicted because of downregulation of photosynthesis (Besford et al., 1998), or that the negative effects will be much less because of acclimation of soil respiration to long-term increases in temperature (Giardina and Ryan, 2000). There is also large uncertainty over whether nitrogen supply will place a severe constraint upon increases in productivity, or increase productivity because of enhanced nitrogen deposition. However, there is little doubt that future increases in the cultivated land area will reduce carbon storage in vegetation. In the past, this has been the major human influence on terrestrial vegetation, and it is likely that it will continue to be so in the future.

Acknowledgements

This study was funded by the UK Department for Environment, Food and Rural Affairs under contract number 1/1/64.

Appendix

To ensure the light used by the two competing tree types did not exceed that available, PAR_0 for each tree type was scaled such that:

$$\text{Scaled PAR}_0 = \text{PAR}_0 \times \frac{1 - e^{-K(\text{LAI}_{\text{BRD}}+\text{LAI}_{\text{NDL}})}}{1 - e^{-K \cdot \text{LAI}_{\text{BRD}}} + 1 - e^{-K \cdot \text{LAI}_{\text{NDL}}}} \tag{A1}$$

PAR incident on the herbaceous layer (PAR_h) was given by,

$$\text{PAR}_h = \text{PAR}_0 \cdot e^{-K(\text{LAI}_{\text{BRD}} + \text{LAI}_{\text{NDL}})} \tag{A2}$$

where BRD and NDL refer to the leaf are index of broadleaved and needle-leaved canopies above the herbaceous layer and PAR_0 is photosynthetically active radiation at the top of the canopy.

Canopy photosynthesis, $A_{w,can}$, for woody vegetation was calculated from

$$A_{w,can} = A \cdot \frac{(1 - e^{-K \cdot \text{LAI}w})}{K} \tag{A3}$$

where A is the rate of net photosynthesis at the top of the layer, K (assumed 0.5) is the extinction coefficient for PAR down the canopy and LAI_w is leaf area

TABLE AI
Vegetation parameters used to model the productivity, growth, and litter disposition of the woody and herbaceous plant components in the global simulations.

Symbol	Description	Value	Units
K	PAR canopy extinction coefficient	0.5	Dimensionless
N_{top}	Canopy top N content	1.3	g(N)/m^2
γ_{f}	Respiration coefficient for foliage	250	kg(C)/kg(C)/s
γ_{s}	Respiration coefficient for stem	1	kg(C)/kg(C)/s
γ_{r}	Respiration coefficient for fine roots	250	kg(C)/kg(C)/s
$\alpha_{\text{h,f}}$	Herbaceous NPP allocation to foliage	0.28	Fraction
$\alpha_{\text{h,s}}$	Herbaceous NPP allocation to stem	0.33	Fraction
$\alpha_{\text{h,r}}$	Herbaceous NPP allocation to fine roots	0.39	Fraction
$\tau_{\text{h,f}}$	Herbaceous foliage turnover	0.8	Yr
$\tau_{\text{h,s}}$	Herbaceous stem turnover	0.8	Yr
$\tau_{\text{h,r}}$	Herbaceous fine root turnover	0.5	Yr
$\alpha_{\text{w,f}}$	Woody NPP allocation to foliage	0.1	Fraction
$\alpha_{\text{w,s}}$	Woody NPP allocation to stem	0.7	Fraction
$\alpha_{\text{w,r}}$	Woody NPP allocation to fine roots	0.2	Fraction
$\tau_{\text{w,r}}$	Woody fine root turnover	0.5	Yr
$\tau_{\text{BRD,f}}$	Broadleaf foliage turnover	1	Yr
$\tau_{\text{NDL,f}}$	Needleleaf foliage turnover	6	Yr
$\tau_{\text{BRD,s}}$	Broadleaf stem turnover	20	Yr
$\tau_{\text{NDL,s}}$	Needleleaf stem turnover	10	Yr
SLA_{BRD}	Broadleaf specific leaf area	36	m^2/kg(C)
SLA_{NDL}	Needleleaf specific leaf area	18	m^2/kg(C)
$f_{\text{w,ag}}$	Fraction of woody stem above-ground	0.7	Fraction
$f_{\text{w,c}}$	Fraction of woody stem coarse	0.7	Fraction

Note. The subscript w, refers to both broadleaf and needleleaf trees whereas BRD and NDL refers to the respective tree type only. K, and N_{top} are the same for the woody and herbaceous layers.

index. Maintenance respiration, R_{m}, was calculated as a constant fraction of canopy photosynthesis:

$$R_{\text{m}} = 0.5 \cdot A_{\text{w,can}}. \tag{A4}$$

Surface temperature, T_{s}, was calculated from:

$$F_{\text{H}} = \frac{\rho\ c_p\ (T_{\text{S}} - T)}{R_{\text{aH}}} \tag{A5}$$

$$F_{\text{H}} = \frac{R_{\text{tH}}}{R_{\text{aH}}} \left(\frac{R_{\text{tE}}\ F_{\text{A}}^{*} - \rho\ \lambda\ D}{\varepsilon\ R_{\text{tH}} + R_{\text{tE}}} \right) \tag{A6}$$

where, F_{H} is the sensible heat flux, ρ is air density, c_p is the isobaric specific heat of air, T is ambient air temperature, R_{aH} is the bulk aerodynamic resistance to heat and

R_{tH} and R_{tE} are the total resistance to heat and water vapour transfer respectively (see Raupach, 1998), F_A^* is the isothermal net available energy, λ is the latent heat of vapourisation, D is the saturation deficit of air ($Q_{sat}(T) - Q$), and ε is the slope of the saturation specific humidity. Evaporation from the surface was then calculated as

$$\text{Evaporation} = \frac{\rho D_S}{R_{tE}} \tag{A7}$$

where D_s is the saturation deficit at the land surface. The soil water holding capacity was related to soil carbon as follows:

$$\text{Soil water capacity} = 0.213 + 0.00227\, C_{soil}. \tag{A8}$$

References

Besford, R. T., Mousseau, M., and Matteucci, G.: 1998, 'Biochemistry, Physiology and Biophysics of Photosynthesis', in Jarvis, P. G. (ed.), *European Forests and Global Change*, Cambridge University Press, Cambridge, pp. 215–235.

Betts, R. A.: 2000, 'Offset of the potential carbon sink from boreal forestation by decreases in surface albedo', *Nature* **408**, 187–190.

Brown, S., Lugo, A. E., and Chapman, J.: 1986, 'Biomass of tropical tree plantations and its implications for the global carbon budget', *Can. J. Forest Res.* **16**, 390–394.

Ciais, P., Tans, P. P., Trolier, M., White, J. W. C., and Francey, R. J.: 1995, 'A large northern-hemisphere terrestrial sink of CO_2 indicated by the $^{13}C/^{12}C$ ratio of atmospheric CO_2', *Science* **269**, 1098–1102.

Comins, H. N. and McMurtrie, R. E.: 1993, 'Long-term response of nutrient-limited forests to CO_2 enrichment – equilibrium behavior of plant-soil models', *Ecol. Appl.* **3**, 666–681.

Cox, P. M., Betts, R. A., Jones, C. D., Spall, S. A., and Totterdell, I. J.: 2000, 'Acceleration of global warming due to carbon-cycle feedbacks in a coupled climate model', *Nature* **408**, 184–187.

Cramer, W.: 2001, 'Global response of terrestrial ecosystem structure and function to CO2 and climate change: Results from six dynamic global vegetation models', *Global Change Biol.* **7**, 357–373.

DeFries, R. S., Field, C. B., Fung, I., Collatz, G. J., and Bounoua, L.: 1999, 'Combining satellite data and biogeochemical models to estimate global effects of human-induced land cover change on carbon emissions and primary productivity', *Global Biogeochem. Cycle* **13**, 803–815.

Dewar, R. C., Medlyn, B. E., and McMurtrie, R. E.: 1999, 'Acclimation of the respiration photosynthesis ratio to temperature: Insights from a model', *Global Change Biol.* **5**, 615–622.

Douville, H., Planton, S., Royer, J. F., Stephenson, D. B., Tyteca, S., Kergoat, L., Lafont, S., and Betts, R. A.: 2000, 'Importance of vegetation feedbacks in doubled-CO_2 climate experiments', *J. Geophys. Res. Atmos.* **105**, 14841–14861.

Fahey, T. J.: 1983, 'Nutrient dynamics of aboveground detritus in lodgepole pine (Pinus contorta ssp. latifolia) ecosystems, southeastern Wyoming', *Ecol. Monogr.* **53**, 51–72.

Farquhar, G. D. and von Caemmerer, S.: 1982, 'Modelling of Photosynthetic Response to Environmental Conditions', in Lange, O. L., Nobel, P., Osmond, C. B. and Ziegler, H. (eds.), *Physiological Plant Ecology II. Water Relations and Carbon Assimilation*, Springer-Verlag, Berlin, pp. 549–587.

Friend, A. D., Stevens, A. K., Knox, R. G., and Cannell, M. G. R.: 1997, 'A process-based, terrestrial biosphere model of ecosystem dynamics (Hybrid v3.0)', *Ecol. Model.* **95**, 249–287.

Friend, A. D. and White, A.: 2000, 'Evaluation and analysis of a dynamic terrestrial ecosystem model under preindustrial conditions at the global scale', *Global Biogeochem. Cycle* **14**, 1173–1190.

Giardina, C. P. and Ryan, M. G.: 2000, 'Evidence that decomposition rates of organic carbon in mineral soil do not vary with temperature', *Nature* **404**, 858–861.

Gifford, R. M.: 1995, 'Whole plant respiration and photosynthesis of wheat under increased CO2 concentration and temperature: Long-term vs short-term distinctions for modelling', *Global Change Biol.* **1**, 385–396.

Gordon, C., Cooper, C., Senior, C. A., Banks, H., Gregory, J. M., Johns, T. C., Mitchell, J. F. B., and Wood, R. A.: 2000, 'The simulation of SST, sea ice extents and ocean heat transports in a version of the Hadley Centre coupled model without flux adjustments', *Clim. Dyn.* **16**, 147–168.

Grier, C. C.: 1978, 'A Tsuga heterophylla – Picea sitchensis ecosystem of coastal Oregon: decomposition and nutriant balance of fallen logs', *Can. J. Forest Res.-Rev. Can. Rech. For.* **18**, 198–206.

Gurney, K. R., Law, R. M., Denning, A. S., Rayner, P. J., Baker, D., Bousquet, P., Bruhwiler, L., Chen, Y. H., Ciais, P., Fan, S., Fung, I. Y., Gloor, M., Heimann, M., Higuchi, K., John, J., Maki, T., Maksyutov, S., Masarie, K., Peylin, P., Prather, M., Pak, B.C., Randerson, J., Sarmiento, J., Taguchi, S., Takahashi, T., and Yuen, C. W.: 2002, 'Towards robust regional estimates of CO_2 sources and sinks using atmospheric transport models', *Nature* **415**, 626–630.

Hao, W. M., Liu, M.-H., and Crutzen, P. J.: 1990, 'Estimates of Annual and Regional Releases of CO2 and Other Trace Gases to the Atmosphere from Fires in the Tropics, Based on the FAO Statistics for the Period 1975–80', in Goldammer, J. G. (ed.), *Fire in the Tropical Biota. Ecosystem Processes and Global Challenges*, Springer-Verlag, Berlin, pp. 440–462.

Houghton, R. A.: 1991, 'Releases of carbon to the atmosphere from degradation of forests in Tropical Asia', *Can. J. For. Res.-Rev. Can. Rech. For.* **21**, 132–142.

Houghton, R. A.: 1995, 'Land-use change and the carbon-cycle', *Global Change Biol.* **1**, 275–287.

Houghton, R. A.: 1999, 'The annual net flux of carbon to the atmosphere from changes in land use 1850–1990', *Tellus Ser. B Chem. Phys. Meteorol.* **51**, 298–313.

Houghton, R. A. and Hackler, J. L.: 1995, *Continental Scale Estimates of the Biotic Carbon Flux from Land Cover Change: 1850 to 1980*, Carbon Dioxide Information Analysis Center, Oak Ridge National Laboratory, Oak Ridge, TN, ORNL/CDIAC-79: 144.

Houghton, R. A. and Hackler, J. L.: 1999, 'Emissions of carbon from forestry and land-use change in tropical Asia', *Global Change Biol.* **5**, 481–492.

Houghton, R. A., Hobbie, J. E., Melillo, J. M., Moore, B., Peterson, B. J., Shaver, G. R., and Woodwell, G. M.: 1983, 'Changes in the carbon content of terrestrial biota and soils between 1860 and 1980: A net release of CO_2 to the atmosphere', *Ecol. Monogr.* **53**, 235–262.

Houghton, R. A., Lefkowitz, D. S., and Skole, D. L.: 1991, 'Changes in the landscape of Latin America between 1850 and 1985. II. Net release of CO_2 to the atmosphere', *Forest Ecol. Manage.* **38**, 173–199.

Houghton, R. A., Lefkowitz, D. S., and Skole, D. L.: 1991, 'Changes in the landscape of Latin-America between 1850 and 1985. 1. Progressive loss of forests', *Forest Ecol. Manage.* **38**, 143–172.

House, J. I., Prentice, I. C., and Le Quere, C.: 2002, 'Maximum impacts of future reforestation or deforestation on atmospheric CO_2', *Global Change Biol.* **8**, 1047–1052.

IPCC: 2000, *Emissions Scenarios. A Special Report of Working Group II of the Intergovernmental Panel on Climate Change*, Cambridge University Press, Cambridge, 612 pp.

John, D. M.: 1973, 'Accumulation and decay of litter and net production of forest in tropical West Africa', *Oikos* **24**, 430–435.

Johns, T. C., Gregory, J. M., Ingram, W. J., Johnson, C. E., Jones, A., Lowe, J. A., Mitchell, J. F. B., Roberts, D. L., Sexton, D. M. H., Stevenson, D. S., Tett, S. F. B., and Woodage, M. J.: 2003, 'Anthropogenic climate change for 1860 to 2100 simulated with the HadCM3 model under updated emissions scenarios', *Clim. Dyn.* **20**, 583–612.

Keeling, C. D., Chin, J. F. S., and Whorf, T. P.: 1996, 'Increased activity of northern vegetation inferred from atmospheric CO_2 measurements', *Nature* **382**, 146–149.

Lugo, A. E., Sanchez, M. J., and Brown, S.: 1986, 'Land use and organic carbon content of some subtropical soils', *Plant Soil* **96**, 185–196.

Martin, M., Dickinson, R. E., and Yang, Z. L.: 1999, 'Use of a coupled land surface general circulation model to examine the impacts of doubled stomatal resistance on the water resources of the American southwest', *J. Clim.* **12**, 3359–3375.

McGuire, A. D., Sitch, S., Clein, J. S., Dargaville, R., Esser, G., Foley, J., Heimann, M., Joos, F., Kaplan, J., Kicklighter, D. W., Meier, R. A., Melillo, J. M., Moore, B., Prentice, I. C., Ramankutty, N., Reichenau, T., Schloss, A., Tian, H., Williams, L. J., and Wittenberg, U.: 2001, 'Carbon balance of the terrestrial biosphere in the twentieth century: Analyses of CO_2, climate and land use effects with four process-based ecosystem models', *Global Biogeochem. Cycle* **15**, 183–206.

Nepstad, D. C., Uhl, C., and Serrao, E. A. S.: 1991, 'Recuperation of a degraded Amazonian landscape – forest recovery and agricultural restoration', *Ambio* **20**, 248–255.

Olson, J. S., Watts, J. A., and Allison, L. J.: 1983, *Carbon in Live Vegetation of Major World Ecosystems*, Oak Ridge National Laboratory, Oak Ridge, Tennessee, 154 pp.

Parton, W. J., Schimel, D. S., Cole, C. V., and Ojima, D. S.: 1987, 'Analysis of factors controlling soil organic matter levels in Great Plains grasslands', *Soil Sci. Soc. Am. J.* **51**, 1173–1179.

Prentice I. C., et al.: 2001, 'The carbon cycle and atmospheric carbon dioxide', in Houghton, J. T., et al. (eds.), *Climate Change 2001: The Scientific Basis: Contribution of Working Group I to the Third Assessment Report of the Intergovernmental Panel on Climate Change*, Cambridge University Press, Cambridge, pp. 183–238.

Ramankutty, N. and Foley, J. A.: 1999, 'Estimating historical changes in global land cover: Croplands from 1700 to 1992', *Global Biogeochem. Cycle* **13**, 997–1027.

Ramankutty, N., Foley, J. A., Norman, J., and McSweeney, K.: 2002, 'The global distribution of cultivable lands: Current patterns and sensitivity to possible climate change', *Global Ecol. Biogeogr.* **11**, 377–392.

Raupach, M. R.: 1998, 'Influences of local feedbacks on land-air exchanges of energy and carbon', *Global Change Biol.* **4**, 477–494.

Reynolds, J. H. and Ford, E. D.: 1999, 'Multi-criteria assessment of ecological process models', *Ecology* **80**, 538–553.

Ryan, M. G.: 1991, 'Effects of climate change on plant respiration', *Ecol. Appl.* **1**, 157–167.

Saldarriaga, J. G.: 1987, 'Recovery following shifting cultivation', in Jordan, C. F. (ed.), *Amazonian Rain Forests*, Springer-Verlag, New York, pp. 24–33.

Sellers, P. J., Berry, J. A., Collatz, G. J., Field, C. B., and Hall, F. G.: 1992, 'Canopy reflectance, photosynthesis, and transpiration. 3. A reanalysis using improved leaf models and a new canopy integration scheme', *Remote Sens. Environ.* **42**, 187–216.

Thornley, J. H. M. and Cannell, M. G. R.: 2000, 'Modelling the components of respiration: Representation and realism', *Ann. Bot.* **85**, 55–67.

Uusivuori, J., Lehto, E., and Palo, M.: 2002, 'Population, income and ecological conditions as determinants of forest area variation in the tropics', *Global Environ. Change Human Policy Dimens.* **12**, 313–323.

van Veen, J. A. and Kuikman, P. J.: 1990, 'Soil structure', *Biogeochemistry* **11**, 213–233.

Voroney, R. P. and Angers, D. A.: 1995, 'Analysis of the Short-Term Effects of Management on Soil Organic Matter Using the CENTURY Model', in Lal, R., Kimble, J., Levine, E. and Stewart, B. A. (eds.), *Soil Management and Greenhouse Effect*, Lewis Publishers, Boca Raton, pp. 113–120.

Waring, R. H., Landsberg, J. J. and Williams, M.: 1998, 'Net primary production of forests: a constant fraction of gross primary production?', *Tree Physiol.* **18**, 129–134.

Waring, R. H. and Running, S. W.: 1998, *Forest Ecosystems: Analysis at Multiple Scales*, Academic Press, San Diego, 370 pp.

White, A., Cannell, M. G. R., and Friend, A. D.: 1999, 'Climate change impacts on ecosystems and the terrestrial carbon sink: a new assessment', *Global Environ. Change Human Policy Dimens.* **9**, S21–S30.

White, A., Cannell, M. G. R., and Friend, A. D.: 2000, 'CO_2 stabilization, climate change and the terrestrial carbon sink', *Global Change Biol.* **6**, 817–833.

White, A., Cannell, M. G. R., and Friend, A. D.: 2000, 'The high-latitude terrestrial carbon sink: A model analysis', *Global Change Biol.* **6**, 227–245.

(Received 13 May 2003; in revised form 1 June 2004)